GEOPHYSICAL RESEARCH LETTERS, VOL. 36, L12201, doi:10.1029/2009GL037600, 2009

A new technique for estimating the thickness of mare basalts in Imbrium Basin

Bradley J. Thomson,[1] Eric B. Grosfils,[2] D. Ben J. Bussey,[1] and Paul D. Spudis[3]

Received 10 February 2009; revised 24 April 2009; accepted 28 April 2009; published 16 June 2009.

[1] The total volume of extrusive volcanism on the Moon provides a basic thermal and geologic constraint, and accurate volume assessments are contingent upon constraining lava flow depths. Here, employing UV-VIS data from the Clementine mission, we estimate mare thickness values in the Imbrium Basin by analyzing ejecta from large (>10 km diameter) impact craters that penetrate (or failed to penetrate) through the mare. Mare thickness values are found to range from at least ~2 km at the basin center to 1.5–2.0 km in the buried ring shelf annulus. This corresponds to a basalt volume of $\sim 1.3 \times 10^6$ km^3, almost a factor of two greater than the volume estimated from partially filled craters alone. Our results indicate that thickness measurements from penetrating craters, combined with minimum estimates from partially filled and non-penetrating craters, provide a more complete picture of the spatial variation of basalt thickness values than could previously be obtained. **Citation:** Thomson, B. J., E. B. Grosfils, D. B. J. Bussey, and P. D. Spudis (2009), A new technique for estimating the thickness of mare basalts in Imbrium Basin, *Geophys. Res. Lett.*, *36*, L12201, doi:10.1029/2009GL037600.

1. Introduction

[2] Approximately 16% (6×10^6 km^2) of the Moon's surface is covered by basaltic lava flows that comprise the lunar maria [*Wilhelms*, 1987]. Although the total areal extent of these lava flows is known, their thicknesses are more difficult to constrain. The question of basalt thickness is an important one, for the total volume of extrusive lunar lava provides a basic constraint on the Moon's thermal and petrogenetic evolution. Measurements of individual flow thickness are somewhat limited [e.g., *Howard et al.*, 1972; *Schaber*, 1973; *Gifford and El-Baz*, 1981; *Hiesinger et al.*, 2002], and these direct measurements only apply to the uppermost lava layers. Indirect techniques for measuring the total accumulated thickness of basalt include using gravity, seismic, or radar data [e.g., *Cooper et al.*, 1974; *Sharpton and Head*, 1982; *Talwani et al.*, 1973]; analyses of craters partially filled with basalt [e.g, *De Hon and Waskom*, 1976; *De Hon*, 1979]; comparisons of lunar basins filled with mare deposits to unfilled basins [*Head*, 1982]; and analyses of impact craters that have completely penetrated the mare [*Andre et al.*, 1979; *Budney and Lucey*, 1998; *Rajmon and Spudis*, 2004].

[3] The thickness estimation technique that provides the highest spatial resolution data is based on craters that have been partially filled with basalt [*De Hon and Waskom*, 1976; *De Hon*, 1979]. In this method, mare thickness is determined from the difference between a partially filled crater's exposed rim height and its estimated original, pre-fill rim height. This technique, however, is not without its drawbacks. Impact degradation of the craters' rim heights may lead to thickness overestimation; it was suggested on this basis that initial estimates made using rim heights may be too high by a factor of two [*Hörz*, 1978]. Alternatively, on the basis of comparison with the unfilled Orientale Basin, it has been suggested that thickness estimates from flooded craters may be too low by a factor of two [*Head*, 1982].

[4] Here we report estimates of lava thicknesses in the Imbrium Basin using 23 large craters >10 km in diameter that have completely penetrated (or failed to penetrate) through the mare. These craters are analyzed with high spatial scale (~100 m/pixel) Clementine UV-VIS multispectral image data to assess the contribution of underlying basement material. Utilization of penetrating craters expands the number of control points available for contouring basalt isopach maps (maps of stratigraphic thickness) and helps provide more robust thickness estimates. Given the inherent non-uniqueness of thickness solutions obtained by the inversion of gravity anomalies, the results of this study can inform these models for locations where an adequate number of control points are available.

2. Method

2.1. Clementine Data Processing

[5] For the craters in Imbrium Basin analyzed in this study, we processed Clementine data from the UVVIS camera to produce maps of estimated iron concentration (wt% FeO) of the surface regolith [*Lucey et al.*, 2000]. Uncertainty values associated with the iron estimates derived using this method are about ±1 wt% based upon calibration of individual Clementine pixels covering the lunar sample-return sites [*Blewett et al.*, 1997; *Lucey et al.*, 1998]. Comparison of the Clementine estimates with iron abundance measurements by Lunar Prospector gamma-ray and neutron spectrometer data reveals a close similarity over most areas of the lunar surface [*Lawrence et al.*, 2002], thus lending confidence to the Clementine-derived iron estimates.

2.2. Crater Excavation Depth

[6] In order to use an impact crater as a subsurface probe, the excavation depth of the crater must be ascertained. As a general rule of thumb, the maximum depth of excavation, H_{exe}, is approximately equal to 1/10 the transient crater diameter (D_t) [*Croft*, 1980; *Melosh*, 1989]. For simple lunar craters (<15 km), the diameter of the transient crater is

[1]Johns Hopkins University Applied Physics Laboratory, Laurel, Maryland, USA.
[2]Geology Department, Pomona College, Claremont, California, USA.
[3]Lunar and Planetary Institute, Houston, Texas, USA.

0094-8276/09/2009GL037600$05.00

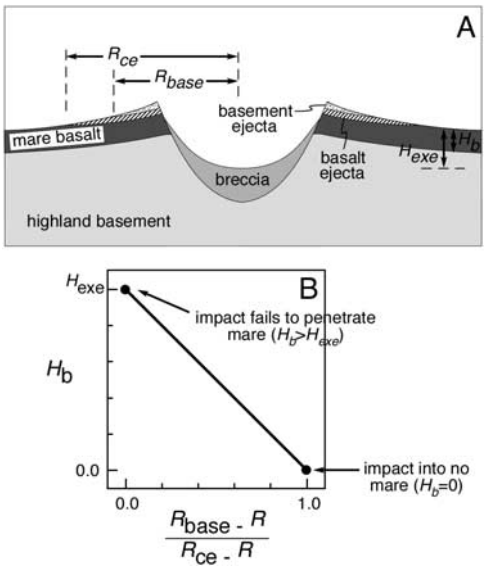

Figure 1. (a) Idealized cross-section of an impact crater than has penetrated the mare/highland interface and exposed basement, low-iron ejecta. R_{ce} is radius of continuous ejecta (as defined in equation (3)), R_{base} is the radius of the low-iron ejecta component, H_{exe} is the excavation depth, and H_b is the thickness of basalt. (b) Plot of basalt thickness (H_b) versus the radial fraction of the continuous ejecta blanket (R_{ce}) occupied by low-iron ejecta (R_{base}). R is the crater's radius. As $R_{base} \rightarrow R_{ce}$, $H_b \rightarrow 0$; as $R_{base} \rightarrow R$, $H_b \rightarrow H_{exe}$.

related to the final crater rim-to-rim diameter (D) by equation (1),

$$D_t = 0.84D. \quad (1)$$

[7] For larger, complex craters (>15 km), the diameter of the transient cavity can be estimated from measurable crater properties using a basic geometric model (see *Melosh*, 1989, p. 143] for further discussion).

$$D_t = \left[\frac{13.5D^3H}{1 + 6\left[1 + \left(D_f/D\right) + \left(D_f/D\right)^2\right]^{-1}}\right]^{0.25} \quad (2)$$

In equation (2), D is the crater's rim-to-rim diameter, H is the crater depth, D_f is the crater's floor diameter, and D_t is the transient crater diameter.

[8] Of the parameters needed in equation (2), the final crater diameter is measured directly from image data. The crater depth and floor diameter (H and D_f) are determined from Lunar Topographic Orthophotomaps where available or are estimated using empirically determined relationships [*Pike*, 1977].

2.3. Ejecta Measurements and Estimation of Basalt Thickness

[9] Measurements of lunar craters [*Moore et al.*, 1974] indicate that the average radius of continuous ejecta (R_{ce}) increases in a regular manner with crater radii (R) as

$$R_{ce} = (2.348 \pm 0.5)\, R^{1.006}. \quad (3)$$

To estimate the thickness of basaltic material penetrated by a crater, we utilize the fact that material from shallower depths within the pre-impact stratigraphy tends to be thrown farther away from the crater rim than material excavated from deeper layers [e.g., *Shoemaker*, 1963; *Stöffler et al.*, 1975]. An inverted stratigraphy is created when material from deeper stratigraphic layers, deposited close to the rim crest, is superposed upon ejecta from shallower depths. We assume that the pre-impact stratigraphic sequence consists of essentially two layers: a layer of mare basalt with horizontal upper and lower boundaries lying atop basement highland material (Figure 1a).

[10] For each of the craters examined in this study, we extracted 36 radial profiles from the estimated iron concentration maps in 10° increments from the crater's center. In each profile, the radial limit of the low FeO basement ejecta was measured and the results were averaged together to determine the mean radial extent of the basement component (R_{base}). Although numerous experimental studies and numerical simulations have investigated impacts into layered targets [e.g., *Stöffler et al.*, 1975; *Senft and Stewart*, 2007], little work has been done that specifically addresses the relationship between radial position of ejecta on the upper surface of the continuous ejecta blanket and depth of excavation in layered targets. Therefore, as a first approximation, we have assumed that the radial fraction of the continuous ejecta blanket occupied by low-iron ejecta is linearly related to the fraction of the maximum excavation depth occupied by basalt (Figure 1b). To test the plausibility of this approximation we measured basalt thickness directly in the near-rim wall slope of the crater Pytheas (see auxiliary material, Figure S1), a measurement that proves unfeasible at most craters due to obscuration by mass wasting and other fill deposits.[1] The measured range of thickness values at Pytheas (0.3–0.8 km) is consistent with the value of 0.44 ± 0.15 km estimated via the penetrating crater method, providing some support for this *ad hoc* assumption. Using this assumption, the thickness of basalt (H_b) can be determined according to the relation:

$$H_b = \left[1 - \left(\frac{R_{base} - R}{R_{ce} - R}\right)\right] H_{exe} \quad (4)$$

We assume that craters lacking a ring of low FeO ejecta did not penetrate completely through the mare, but such craters remain useful as they provide constraints on the minimum basalt thickness (i.e., in equation (4), if $R_{base} \leq R$, $H_b \geq H_{exe}$).

[11] One potential concern with our general approach is that mixing of crater ejecta may obscure the signal, either from ballastic sedimentation [*Oberbeck*, 1975] or later regolith gardening [e.g., *Gault et al.*, 1974]. However, as indicated by the example given in Figure 2, the penetrating craters analyzed in this study show an abrupt, step-like discontinuity within their continuous ejecta blankets that marks the terminus of low FeO ejecta. It is unlikely that

[1] Auxiliary materials are available in the HTML. doi:10.1029/2009GL037600.

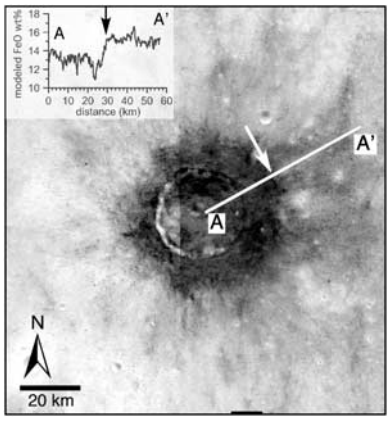

Figure 2. Estimated iron concentration map of the crater Timocharis (crater diameter = 33 km) derived from Clementine UV-VIS data [*Lucey et al.*, 2000]. Radial profile A-A′ shows distinct step (arrow) from low iron ejecta inferred to represent sub-mare basement material to higher iron ejecta.

these sharp discontinuities would be preserved if mixing were a major issue.

3. Results

[12] We examined all 23 craters on Mare Imbrium >10 km in diameter (Table 1). As indicated by their surrounding halos of low FeO ejecta (e.g., Figure 2), six craters (Aristillus, Autolycus, Brayley B, Euler, Pytheas, and Timocharis) clearly penetrate the mare and excavate low iron basement material. Nine others lack a low iron ejecta component (Table 1) and we infer that they failed to penetrate the mare/highland interface and thus yield only minimum estimates of basalt thickness. Six craters (Table 1) are partially filled with basalt. Finally, two additional craters (Table 1) have a low iron component exposed in their central peak regions but not in their ejecta. This suggests that the mare/highland interface is close to, but below, these craters' maximum excavation depths, and that exposures of basement material were brought up to the surface due to rebound during the modification stage of crater formation. *Cintala and Grieve* [1998] used data from 12 lunar craters to derive an empirical relationship between the magnitude of structural uplift (u_s) and crater diameter of $u_s = 0.022D^{1.45}$, yielding an average uplift depth of about 0.1 D. This value agrees well with studies of the depth of structural uplift in complex terrestrial craters [e.g., *Grieve and Therriault*, 2004]. Using these uplift estimates, for craters with low FeO central peak regions, the depth of basalt can be generally constrained to be greater than the excavation depth (H_{exe}) but less than $H_{exe} - 0.1\ D$.

[13] Measured thickness values from this study were combined with thickness data points derived from partially flooded craters to create the basalt isopach thickness map in Figure 3a. A simplified version of the previous isopach map made using partially flooded crater data alone [*De Hon*, 1979] is given in Figure 3b for comparison.

4. Discussion

[14] In comparing the revised and original map of mare basalt thickness (Figures 3a and 3b, respectively), it is apparent that much of the basic spatial pattern remains consistent. Mare Imbrium consists of a circular central thick lens that is surrounded by an annular zone of thinner basalt (some of which is presumably located over a buried Imbrium Basin ring and ring shelf [*Spudis*, 1993]). Outside

Table 1. Imbrium Craters

Crater	Latitude (deg N)	Longitude (deg W)	Diameter D (km)	D_t[a] (km)	H_b, Basalt Thickness[b] (km)	Comment	Time-Stratigraphic System[c]
Archimedes	29.7	4.0	82.0	51.5	na	flooded crater	Imbrian
Aristillus	33.9	−1.2	55.0	36.6	1.58 ± 0.36	penetrated mare	Copernican
Autolycus	30.7	−1.5	39.0	27.3	1.17 ± 0.25	penetrated mare	Copernican
Brayley B	20.8	34.3	10.0	8.4	na	penetrated mare, but ejecta obscured	Eratosthenian
C. Herschel	34.5	31.2	13.0	10.9	>1.09 ± 0.1	failed to penetrate	Eratosthenian
Carlini	33.7	24.1	10.0	8.4	>0.84 ± 0.08	failed to penetrate	Imbrian
Cassini	40.2	−4.6	56.0	37.2	na	flooded crater	Imbrian
Cassini A	40.5	−4.8	15.0	12.1	>1.21 ± 0.1	failed to penetrate	Copernican
Delisle	29.9	34.6	25.0	18.7	>1.9 ± 0.2 (<3.7)	low FeO interior	Imbrian
Diophantus	27.6	34.3	17.0	13.5	>1.35 ± 0.1	failed to penetrate	Imbrian
Euler	23.3	29.2	27.0	20.0	1.04 ± 0.24	penetrated mare	Copernican
Heis	32.4	31.9	14.0	11.8	>1.18 ± 0.1	failed to penetrate	Eratosthenian
Helicon	40.4	23.1	24.0	18.1	>1.81 ± 0.2	failed to penetrate, partly flooded	Imbrian
Kirch	39.2	5.6	11.0	9.2	>0.92 ± 0.09	failed to penetrate	Eratosthenian
Lambert	25.8	21.0	30.0	20.7	>2.0 ± 0.2 (<4.1)	low FeO interior	Eratosthenian
Lambert R	23.9	20.6	55.0	36.6	na	flooded crater	Imbrian
Le Verrier	40.3	20.6	20.0	15.5	>1.55 ± 0.2	failed to penetrate	Eratosthenian
Natasha	20.0	31.3	12.0	10.1	na	flooded crater	Imbrian
Piazzi Smyth	41.9	3.2	13.0	10.9	>1.10 ± 0.1	failed to penetrate	Eratosthenian
Pytheas	20.5	20.6	20.0	15.5	0.44 ± 0.15	penetrated mare	Eratosthenian
Spurr	27.9	1.2	13.0	10.9	na	flooded crater	Imbrian
Timocharis	26.7	13.1	33.0	23.7	0.91 ± 0.19	penetrated mare	Copernican
Wallace	20.3	8.7	26.0	19.3	na	flooded crater	Imbrian

[a] D_t = transient crater diameter, values derived from equation (1) or (2) as appropriate.
[b] H_b = basalt thickness values derived from equation (4); na means not available.
[c] Based on 1:1,000,000 scale USGS lunar geologic maps I-462, I-463, I-465, I-602, and I-666.

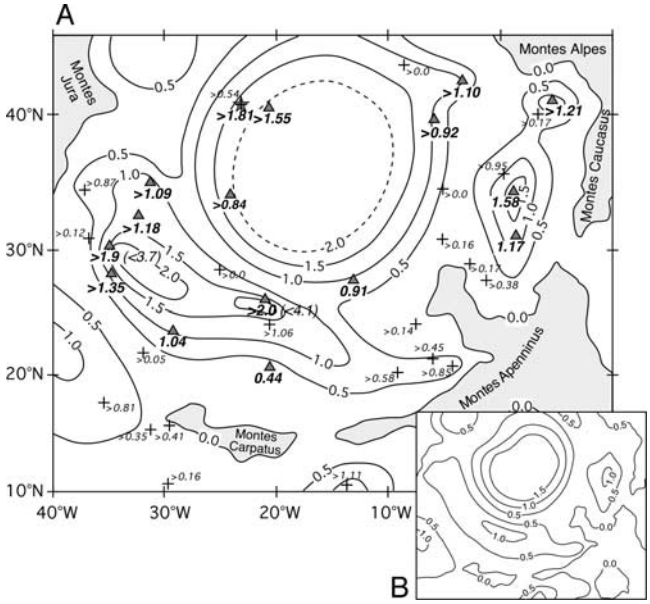

Figure 3. (a) Basalt isopach map of Mare Imbrium. Filled triangles represent craters examined in this study, crosses represent locations of partially flooded craters examined previously [*De Hon*, 1979]. Helicon Crater is marked by filled star. All data labels are given in km; contour interval is 0.5 km. The position of the 2.0 km contour is not well constrained and is depicted with a dashed line to reflect this uncertainty. (b) Simplified basalt isopach map of Mare Imbrium determined from partially flooded craters (after *De Hon* [1979], reprinted by permission of Elsevier).

this annulus, the thickness increases before decreasing to zero at the basin margins. The principal difference between the two maps is that the thickness values for the craters measured in this study are in excess of 0.5 km greater than the thickness values determined from partially flooded craters alone. Mare basalts in the central portion of the basin may exceed 2.0 km in depth (instead of the previously reported 1.5 km), and the regions of closed contours in the southwest and eastern portions of the basin have increased maximum values from 1.0 to 1.5–2.0 km. This 0.5 km excess of thickness values is greater than the uncertainty associated with individual thickness estimates (Table 1).

[15] The one location where the results of our study directly contradict flooded crater thickness estimates is at the crater Helicon (Figure 3a, crater marked with gray star centered at 40.4°N, 23.1°W). The estimated iron concentration map of this crater confirms that it is partially flooded with mare basalts, consistent with the previous thickness estimate of 0.54 km [*De Hon*, 1979]. Yet although the ejecta blanket of Helicon is partially obscured by younger lava flows, no trace of low FeO highland basement material is evident in the proximal ejecta. Therefore, it appears that Helicon Crater impacted onto an intermediate basalt surface and was then embayed and partially flooded by later lava flows. The thickness value of 0.54 km likely represents the thickness of the most recent episodes of mare volcanism in this region, while the cumulative thickness of basalt exceeds the crater's excavation depth (>1.81 km).

[16] The example of Helicon Crater illustrates that partially flooded craters, at least in this study area, typically reflect minimum thickness values. Partially flooded craters only record the thickness of mare fill emplaced after each crater formed; this study indicates that the total basalt thickness may be substantially greater if the flooded craters postdate early mare fill. On balance, the results from our study do not support the assertion that basalt thickness estimates obtained from partially flooded craters were systematically overestimated [*Hörz*, 1978]. While the results support the general approach of using basin scaling to constrain thickness values [e.g., *Head*, 1982], our understanding of Imbrium Basin is advanced significantly by using a network of individual thickness estimates that are more sensitive to small-scale variability.

[17] Our analysis indicates that Mare Imbrium has a total volume of basalt equal to about 1.3×10^6 km^3, a value which is almost a factor of two greater (92%) than the value based on the results of flooded craters (6.8×10^5 km^3, see Figure S2). Measurements of basalt depth in the basin ring shelf area are well constrained by multiple data points in this study and have a correspondingly high degree of confidence associated with them. The total thickness of fill at the center of the basin, however, still cannot be directly constrained using the methods employed in this study – a value of 2.0 km is assumed here for the innermost radius of 200 km. This is substantially less than the 9.25 km inferred from Apollo gravity data [*Solomon and Head*, 1980], although this value may be an overestimate since it does not account for an uplifted plug of mantle material [*Wise and Yates*, 1970; *Neumann et al.*, 1996]. Estimates of the basin center fill depth based on Clementine altimetry range from 3–4 km [*Spudis and Adkins*, 1996] to 5.24 km [*Williams and Zuber*, 1998]. If central thicknesses in the range of 3.0 to 5.24 km are assumed instead of 2.0 km, the resulting total volume of basalt in Imbrium (about 1.4 to 1.7 $\times 10^6$ km^3) is largely unchanged, increasing by only 8–30%.

[18] The total volume of extruded basalt in Imbrium Basin provides, at least in part, important thermal and geophysical constraints for the Moon. While extrapolating our results to a blanket assessment of the global inventory of lunar volcanism is premature (until thickness estimates for other mare are re-assessed as well), recent estimates of the total basalt volume of 2×10^6 km^3 [*Wieczorek et al.*, 2006] are inconsistent with our value for Imbrium alone (1.3×10^6 km^3). Our data suggest higher net eruption volumes, consistent with some earlier global predictions [e.g., *Head and Wilson*, 1992], and hence a greater degree of thermal activity for the Moon.

References

Andre, C. G., et al. (1979), Mare basalt depths from orbital x-ray data, *Lunar Planet. Sci.*, *X*, abstract 1014.

Blewett, D. T., P. G. Lucey, B. R. Hawke, and B. L. Jolliff (1997), Clementine images of the lunar sample-return stations: Refinement of FeO and TiO_2 mapping techniques, *J. Geophys. Res.*, *102*(E7), 16,319–16,325.

Budney, C. J., and P. G. Lucey (1998), Basalt thickness in Mare Humorum: The crater excavation method, *J. Geophys. Res.*, *103*(E7), 16,855–16,870.

Cintala, M. J., and R. A. F. Grieve (1998), Scaling impact-melt and crater dimensions: Implications for the lunar cratering record, *Meteorit. Planet. Sci.*, *33*, 889–912.

Cooper, M. R., R. L. Kovach, and J. S. Watkins (1974), Lunar near-surface structure, *Rev. Geophys.*, *12*, 291–308.

Croft, S. K. (1980), Cratering flow fields: Implications for the excavation and transient expansion stages of crater formation, *Proc. Lunar Planet. Sci.*, *11*, 2347–2378.

De Hon, R. A. (1979), Thickness of western mare basalts, *Proc. Lunar Planet. Sci. Conf.*, *10*, 2935–2955.

De Hon, R. A., and J. D. Waskom (1976), Geologic structure of the eastern mare basins, *Proc. Lunar Planet. Sci. Conf.*, *7*, 2729–2746.

Gault, D. E., et al. (1974), Mixing of the lunar regolith, *Proc. Lunar Planet. Sci. Conf.*, *3*, 2365–2386.

Gifford, A. W., and F. El-Baz (1981), Thicknesses of lunar mare flow fronts, *Moon Planets*, *24*, 391–398.

Grieve, R. A. F., and A. M. Therriault (2004), Observations at terrestrial impact structures: Their utility in constraining crater formation, *Meteorit. Planet. Sci.*, *39*, 199–216.

Head, J. W. (1982), Lava flooding of ancient planetary crusts: Geometry, thickness, and volumes of flooded lunar impact basins, *Moon Planets*, *26*, 61–88.

Head, J. W., and L. Wilson (1992), Lunar mare volcanism: Stratigraphy, eruption conditions, and the evolution of secondary crusts, *Geochim. Cosmochim. Acta*, *56*, 2155–2175.

Hiesinger, H., J. W. Head III, U. Wolf, R. Jaumann, and G. Neukum (2002), Lunar mare basalt flow units: Thicknesses determined from crater size-frequency distributions, *Geophys. Res. Lett.*, *29*(8), 1248, doi:10.1029/2002GL014847.

Hörz, F. (1978), How thick are the lunar mare basalts?, *Proc. Lunar Planet. Sci. Conf.*, *9*, 3311–3331.

Howard, K. A., et al. (1972), Geology of Hadley Rille, *Proc. Lunar Sci. Conf.*, *2*, 1–14.

Lawrence, D. J., W. C. Feldman, R. C. Elphic, R. C. Little, T. H. Prettyman, S. Maurice, P. G. Lucey, and A. B. Binder (2002), Iron abundances on the lunar surface as measured by the Lunar Prospector gamma-ray and neutron spectrometers, *J. Geophys. Res.*, *107*(E12), 5130, doi:10.1029/2001JE001530.

Lucey, P. G., D. T. Blewett, and B. R. Hawke (1998), Mapping the FeO and TiO_2 content of the lunar surface with multispectral imagery, *J. Geophys. Res.*, *103*(E2), 3679–3699.

Lucey, P. G., D. T. Blewett, and B. L. Jolliff (2000), Lunar iron and titanium abundance algorithms based on final processing of Clementine ultraviolet-visible images, *J. Geophys. Res.*, *105*(E8), 20,297–20,305.

Melosh, H. J. (1989), *Impact Cratering: A Geologic Process*, 245 pp., Oxford Univ. Press, New York.

Moore, H. J., et al. (1974), Multiringed basins—Illustrated by Orientale and associated features, *Proc. Lunar Sci. Conf.*, *5*, 71–100.

Neumann, G. A., M. T. Zuber, D. E. Smith, and F. G. Lemoine (1996), The lunar crust: Global structure and signature of major basins, *J. Geophys. Res.*, *101*(E7), 16,841–16,843.

Oberbeck, V. R. (1975), The role of ballistic erosion and sedimentation in lunar stratigraphy, *Rev. Geophys.*, *13*, 337–362.

Pike, R. J. (1977), Apparent depth/apparent diameter relation for lunar craters, *Proc. Lunar Sci. Conf.*, *8*, 3427–3436.

Rajmon, D., and P. Spudis (2004), Distribution and stratigraphy of basaltic units in maria Tranquillitatis and Fecunditatis: A Clementine perspective, *Meteorit. Planet. Sci.*, *39*, 1699–1720.

Schaber, G. G. (1973), Lava flows in Mare Imbrium: Geologic evaluation from Apollo orbital photography, *Proc. Lunar Sci. Conf.*, *4*, 73–92.

Senft, L. E., and S. T. Stewart (2007), Modeling impact cratering in layered surfaces, *J. Geophys. Res.*, *112*, E11002, doi:10.1029/2007JE002894.

Sharpton, V. L., and J. W. Head III (1982), Stratigraphy and structural evolution of southern Mare Serenitatis: A reinterpretation based on Apollo Lunar Sounder Experiment data, *J. Geophys. Res.*, *87*(B13), 10,983–10,998.

Shoemaker, E. M. (1963), Impact mechanics at Meteor Crater, Arizona, in *The Moon, Meteorites and Comets*, edited by B. M. Middlehurst and G. P. Kuiper, pp. 301–336, Univ. of Chicago Press, Chicago, Ill.

Solomon, S. C., and J. W. Head (1980), Lunar mascon basins: Lava filling, tectonics, and evolution of the lithosphere, *Rev. Geophys.*, *18*, 107–141.

Spudis, P. D. (1993), *The Geology of Multi-Ring Impact Basins*, 263 pp., Cambridge Univ. Press, Cambridge, U. K.

Spudis, P. D., and C. D. Adkins (1996), Morphometry of basins on the Moon: New results from Clementine laser altimetry, *Lunar Planet. Sci.*, *XXVIII*, abstract 1627.

Stöffler, D., D. E. Gault, J. Wedekind, and G. Polkowski (1975), Experimental hypervelocity impact into quartz sand: Distribution and shock metamorphism of ejecta, *J. Geophys. Res.*, *80*(29), 4062–4077.

Talwani, M., G. Thompson, B. Dent, H.-G. Kahle, and S. Buck (1973), Traverse Gravimeter Experiment, in Apollo 17: Preliminary Science Report, edited by R. A. Parker et al., *NASA Spec. Pub. 330*, pp. 13-1 to 13-13, NASA, Washington, D.C.

Wieczorek, M. A., et al. (2006), The constitution and structure of the lunar interior, in *New Views of the Moon*, edited by B. L. Jolliff et al., pp. 221–364, Mineral. Soc. of Am., Chantilly, Va.

Wilhelms, D. E. (1987), The geologic history of the Moon, *U.S. Geol. Surv. Prof. Pap.*, *1348*, 302 pp.

Williams, K. K., and M. T. Zuber (1998), Measurement and analysis of lunar basin depths from Clementine altimetry, *Icarus*, *131*, 107–122.

Wise, D. U., and M. T. Yates (1970), Mascons as structural relief on a lunar Moho, *J. Geophys. Res.*, *75*(2), 261–268.

D. B. J. Bussey and B. J. Thomson, Johns Hopkins University Applied Physics Laboratory, 11100 Johns Hopkins Road, Laurel, MD 20723, USA. (bradley.thomson@jhuapl.edu)

E. B. Grosfils, Geology Department, Pomona College, 185 E 6th Street, Claremont, CA 91711, USA.

P. D. Spudis, Lunar and Planetary Institute, 3600 Bay Area Boulevard, Houston, TX 77058, USA.